ABSOLUTE LOCALIZATION OF FAST MOBILE ROBOTS BASED ON AN ANGLE MEASUREMENT TECHNIQUE

U. D. HANEBECK and G. SCHMIDT

Department for Automatic Control Engineering, Technische Universität München, 80290 München, Germany. E-mail: {hnb, gs}@lsr.e-technik.tu-muenchen.de

Abstract. This paper presents an algorithm for absolute localization of mobile robots, which are equipped with an onboard–device making angular measurements on the location of known but undistinguishable landmarks. A simple *linear* solution for the robot position given $N \geq 3$ angle measurements is derived. The associated uncertainties in both landmark positions and angle measurement are modeled as unknown but bounded in amplitude. Experiments with the set theoretic estimator demonstrate its simplicity and effectiveness in real–world applications.

Key Words. Angular measurement; Nonlinear filtering; Recursive Estimation; Set theory; Vehicles

1. INTRODUCTION

This paper introduces an approach for estimating the absolute posture (position x, y; orientation ψ) of a fast mobile robot on a planar surface. The algorithm processes onboard measurements of angular locations of known landmarks. Both, initialization of the robot posture and recursive in–motion posture estimation is considered.

For initialization purposes, a set of angles measured with respect to the robot coordinate system needs to be paired with a subset of the undistinguishable landmarks. In (Wiklund *et al.*, 1988), an enumerative scheme has been reported for pairing the first three angles with landmarks. The remaining angles are used for plausibility tests. Several solutions for calculating the posture given the correct association of measured angles with landmarks have been reported. Sutherland and Thompson (1994), Tsumura *et al.* (1993), and Wiklund *et al.* (1988) consider only triples of landmarks. For the case of more than three landmarks some authors average triple solutions, others use iterative techniques. Betke and Gurvits (1994) supply a closed–form solution for N angles, which does not consider uncertainties. In this paper, a more efficient association algorithm is developed. It discards false measurements, is fast, and is further accelerated by incorporating prior knowledge. Furthermore, it takes advantage of a simple closed–form solution, which consists of a set of $N-1$ *linear* equations for the vehicle position, Sect. 3. An error propagation analysis may be performed, which considers uncertainties in both landmark positions and angle measurement.

If the vehicle velocity is high compared to the angle measurement rate, posture estimates can be sequentially updated by newly incoming bearing measurements. In (Wiklund *et al.*, 1988), a Kalman filtering scheme is introduced for this purpose, which is based on a kinematic vehicle model. White Gaussian random processes are used as uncertainty models; no dead–reckoning information is considered. Nishizawa *et al.* (1995) also use a statistical method to fuse sensor data with dead–reckoning data. In this paper, a set theoretic modeling of the predominantly arising non–random uncertainties is presented. A recursive set theoretic estimator is proposed for the fusion of every measured angle with a posture prediction that is obtained by propagating the previous estimate by means of dead–reckoning data. Sect. 4 suggests an implementation with real–time capabilities. Experiments demonstrate the benefits of the developed localization algorithm in Sect. 5.

2. PROBLEM FORMULATION

Consider a pool of M *undistinguishable* landmarks in a two–dimensional world or map. The positions of the landmarks x_i^{LM}, y_i^{LM}, $i = 0, 1, \ldots, M-1$ in a reference coordinate system are assumed to be known with additive bias errors, which are of course unknown.

$$\begin{aligned} \hat{x}_i^{\mathrm{LM}} &= \tilde{x}_i^{\mathrm{LM}} + \Delta x_i^{\mathrm{LM}} \\ \hat{y}_i^{\mathrm{LM}} &= \tilde{y}_i^{\mathrm{LM}} + \Delta y_i^{\mathrm{LM}} \quad . \end{aligned} \tag{1}$$

True values of $*$ will be denoted as $\tilde{*}$, nominal or estimated values as $\hat{*}$. The errors of every landmark are assumed to be confined to an ellipsoidal

set given by

$$\begin{pmatrix} \Delta x_i^{\mathrm{LM}} \\ \Delta y_i^{\mathrm{LM}} \end{pmatrix}^T (\mathbf{C}_i^{\mathrm{LM}})^{-1} \begin{pmatrix} \Delta x_i^{\mathrm{LM}} \\ \Delta y_i^{\mathrm{LM}} \end{pmatrix} \leq 1 . \qquad (2)$$

Possible correlation of errors for different landmarks is ignored. The robot is capable of determining the angular locations of these landmarks with respect to its coordinate system. Individual landmarks do not necessarily have to be distinguished. The angle measurements are corrupted by additive noise, i.e., $\hat{\alpha} = \tilde{\alpha} + \Delta\alpha$, where $\Delta\alpha$ is assumed to be bounded in amplitude according to $|\Delta\alpha| < \delta_\alpha$. To account for possible occlusion of landmarks in non–convex rooms, partitioning walls are added to the map. The landmarks are ordered in the map so that the robot detects the subset of unoccluded landmarks in that order when scanning counterclockwise.

3. DETERMINING THE INITIAL POSTURE

This section is concerned with (re–) initializing the robot posture $\underline{z} = (x, y, \psi)^T$ when only very little prior knowledge is available. A priori information is specified by confining the posture to an ellipsoidal set $\Omega_{\text{a-priori}}$. M landmarks are available and $3 < N < M$ angles α_i, $i = 0, 1, \ldots, N-1$ have been measured. The association, i.e., the list of pairings of measured angles to landmarks is initially unknown. Inspired by the interpretation–tree (IT) method in (Drumheller, 1987), the association search is kept from becoming intractable by approaching it in two steps: In the first step, for every measured angle α_i the set of visible landmarks from $\Omega_{\text{a-priori}}$ is determined. In the second step, these visibility constraints are exploited for pruning the IT. Thus, only a small portion of all associations needs to be generated and tested.

Step 1: The projection of $\Omega_{\text{a-priori}}$ onto the x/y-plane is examined at polar grid points $x(r,\theta)$, $y(r,\theta)$ for some r, θ. We define a visibility matrix $\mathcal{V}$ with dimensions N by M. The elements $\mathcal{V}_{ij}$ are boolean variables which are TRUE, if the single measured angle α_i may be caused by landmark j. A visibility test is performed for every grid point $x(r,\theta)$, $y(r,\theta)$. If the landmark j is visible, i.e., when the straight line from the considered grid point $x(r,\theta)$, $y(r,\theta)$ to x_j^{LM}, y_j^{LM} does not intersect any partitioning walls, a hypothetical angle α_{hyp} is calculated. The minimum and maximum angles at $x(r,\theta)$, $y(r,\theta)$ within $\Omega_{\text{a-priori}}$ are denoted as ψ_{LOW}, ψ_{HIGH} respectively. α_i may then be caused by landmark j, if $\alpha_i + \psi_{\mathrm{LOW}} < \alpha_{hyp} < \alpha_i + \psi_{\mathrm{HIGH}}$. If row i of $\mathcal{V}$ does not contain any TRUE value, α_i has been identified as false measurement. Row i is then removed from $\mathcal{V}$ and the number of measurements N is decremented.

Step 2: Only those candidate associations are generated that do not violate the visibility constraints represented by $\mathcal{V}$ and that also follow the ordering assumption. Erroneous measurements are handled efficiently by adopting the "least bad data" constraint proposed in (Grimson and Lozano-Pérez, 1985). For a specific association, a tentative position x_T, y_T is calculated and checked for compatibility with the error bounds, the posture constraint $\Omega_{\text{a-priori}}$, and the requirements for joint visibility of all landmarks involved.

Tentative postures are quickly calculated by use of a closed–form solution. The corresponding set of $N-1$ *linear* equations for the position is derived next. Define γ_i as the difference between two consecutive angles α_i and α_{i+1}, i.e., $\gamma_i = \alpha_{i+1} - \alpha_i$ or

$$\begin{aligned} \gamma_i = &\operatorname{atan2}(x_{i+1}^{\mathrm{LM}} - x, y_{i+1}^{\mathrm{LM}} - y) \\ &- \operatorname{atan2}(x_i^{\mathrm{LM}} - x, y_i^{\mathrm{LM}} - y) . \end{aligned} \qquad (3)$$

Application of trigonometric identities leads to

$$\tan(\gamma_i) = \frac{\frac{y_{i+1}^{\mathrm{LM}} - y}{x_{i+1}^{\mathrm{LM}} - x} - \frac{y_i^{\mathrm{LM}} - y}{x_i^{\mathrm{LM}} - x}}{1 + \frac{y_{i+1}^{\mathrm{LM}} - y}{x_{i+1}^{\mathrm{LM}} - x} \cdot \frac{y_i^{\mathrm{LM}} - y}{x_i^{\mathrm{LM}} - x}} , \qquad (4)$$

which may be rewritten as

$$\begin{aligned} &y_{i+1}^{\mathrm{LM}} y_i^{\mathrm{LM}} + x_{i+1}^{\mathrm{LM}} x_i^{\mathrm{LM}} + \cot(\gamma_i)[x_{i+1}^{\mathrm{LM}} y_i^{\mathrm{LM}} - y_{i+1}^{\mathrm{LM}} x_i^{\mathrm{LM}}] \\ &= \begin{pmatrix} \cot(\gamma_i)[y_i^{\mathrm{LM}} - y_{i+1}^{\mathrm{LM}}] + x_{i+1}^{\mathrm{LM}} + x_i^{\mathrm{LM}} \\ \cot(\gamma_i)[x_{i+1}^{\mathrm{LM}} - x_i^{\mathrm{LM}}] + y_{i+1}^{\mathrm{LM}} + y_i^{\mathrm{LM}} \end{pmatrix}^T \begin{pmatrix} x \\ y \end{pmatrix} \\ &- \begin{pmatrix} x & y \end{pmatrix} \begin{pmatrix} x \\ y \end{pmatrix} \end{aligned} \qquad (5)$$

for $i = 0, 1, \ldots, N-1$. Index operations are performed modulo–N, i.e., $i+1 = 0$ for $i = N-1$. Subtracting from every equation its follower equation yields a system of $N-1$ equations that are *linear* in x and y, i.e., $\underline{z} = \mathbf{H}(x,y)^T + \underline{e}$ with $\underline{z} = (z_0, z_1, \ldots, z_{N-2})^T$, $\mathbf{H} = (\underline{h}_0^T, \underline{h}_1^T, \ldots, \underline{h}_{N-2}^T)^T$, $\underline{h}_i = (h_i^x, h_i^y)^T$, and error $\underline{e} = (e_0, e_1, \ldots, e_{N-2})^T$. The corresponding elements are given by

$$\begin{aligned} z_i = &y_{i+1}^{\mathrm{LM}} y_i^{\mathrm{LM}} + x_{i+1}^{\mathrm{LM}} x_i^{\mathrm{LM}} - y_{i+2}^{\mathrm{LM}} y_{i+1}^{\mathrm{LM}} - x_{i+2}^{\mathrm{LM}} x_{i+1}^{\mathrm{LM}} \\ &+ \cot(\gamma_i)[x_{i+1}^{\mathrm{LM}} y_i^{\mathrm{LM}} - y_{i+1}^{\mathrm{LM}} x_i^{\mathrm{LM}}] \\ &- \cot(\gamma_{i+1})[x_{i+2}^{\mathrm{LM}} y_{i+1}^{\mathrm{LM}} - y_{i+2}^{\mathrm{LM}} x_{i+1}^{\mathrm{LM}}] \\ h_i^x = &\cot(\gamma_i)[y_i^{\mathrm{LM}} - y_{i+1}^{\mathrm{LM}}] + x_i^{\mathrm{LM}} \\ &- \cot(\gamma_{i+1})[y_{i+1}^{\mathrm{LM}} - y_{i+2}^{\mathrm{LM}}] - x_{i+2}^{\mathrm{LM}} \\ h_i^y = &\cot(\gamma_i)[x_{i+1}^{\mathrm{LM}} - x_i^{\mathrm{LM}}] + y_i^{\mathrm{LM}} \\ &- \cot(\gamma_{i+1})[x_{i+2}^{\mathrm{LM}} - x_{i+1}^{\mathrm{LM}}] - y_{i+2}^{\mathrm{LM}} . \end{aligned} \qquad (6)$$

Once x, y are known, ψ can be obtained immediately. To enhance the quality of the solution, an error propagation analysis is performed, which is outside the scope of this paper.

4. IN–MOTION LOCALIZATION

The robot is assumed to be equipped with an odometry which mainly suffers from amplitude–bounded noise sources, that may be strongly correlated or even deterministic. A dead–reckoning system calculates sets of relative posture compatible with the a priori given error bounds. Recursive set theoretic estimation is performed by combining information from an angle measurement at time k with a propagated version of the previous posture estimate at time $k-1$. Ellipsoidal bounding sets (EBS) are used for all operations to achieve real–time capabilities.

4.1. *Propagation*

The result of the fusion process at time $k-1$ is represented by the EBS

$$\Omega^E_{k-1} = \{\underline{z}^E_{k-1} : \\ (\underline{z}^E_{k-1} - \hat{\underline{z}}^E_{k-1})^T \left(\mathbf{C}^E_{k-1}\right)^{-1} (\underline{z}^E_{k-1} - \hat{\underline{z}}^E_{k-1}) \leq 1\}. \tag{7}$$

The dead–reckoning system supplies the set of relative postures with respect to $\underline{z}^E_{k-1}$, henceforth denoted as

$$\Omega^\Delta_k = \{\underline{z}^\Delta_k : \\ (\underline{z}^\Delta_k - \hat{\underline{z}}^\Delta_k)^T \left(\mathbf{C}^\Delta_k\right)^{-1} (\underline{z}^\Delta_k - \hat{\underline{z}}^\Delta_k) \leq 1\} \ . \tag{8}$$

The exact set of absolute postures predicted by the dead–reckoning system is then given by

$$\Omega^P_k = \{\underline{z}^P_k : \underline{z}^P_k = \mathbf{I}\underline{z}^E_{k-1} + \mathbf{B}_k \underline{z}^\Delta_k\} \ , \tag{9}$$

with $\underline{z}^E_{k-1} \in \Omega^E_{k-1}$, $\underline{z}^\Delta_k \in \Omega^\Delta_k$, $\mathbf{I}$ the identity matrix, and

$$\mathbf{B}_k = \begin{pmatrix} \cos(\psi^E_{k-1}) & -\sin(\psi^E_{k-1}) & 0 \\ \sin(\psi^E_{k-1}) & \cos(\psi^E_{k-1}) & 0 \\ 0 & 0 & 1 \end{pmatrix} \ . \tag{10}$$

Unfortunately, Ω^P_k is not in general an ellipsoid. Linearizing (9) around the nominal values yields

$$\underline{z}^P_k - \hat{\underline{z}}^P_k \approx \mathbf{J}^E_k (\underline{z}^E_{k-1} - \hat{\underline{z}}^E_k) + \hat{\mathbf{B}}_k (\underline{z}^\Delta_k - \hat{\underline{z}}^\Delta_k) \tag{11}$$

with the Jacobian

$$\mathbf{J}^E_k = \begin{pmatrix} 1 & 0 & -(\hat{y}^P_k - \hat{y}^E_{k-1}) \\ 0 & 1 & (\hat{x}^P_k - \hat{x}^E_{k-1}) \\ 0 & 0 & 1 \end{pmatrix} \ . \tag{12}$$

Ω^P_k may then be approximated as the EBS for the Minkowski sum of the two ellipsoids in (11)

$$\Omega^P_k \approx \{\underline{z}^P_k : \\ (\underline{z}^P_k - \hat{\underline{z}}^P_k) \left(\mathbf{C}^P_k\right)^{-1} (\underline{z}^P_k - \hat{\underline{z}}^P_k)^T \leq 1\} \ , \tag{13}$$

with center $\hat{\underline{z}}^P_k$ and $\mathbf{C}^P_k$ given by

$$\hat{\underline{z}}^P_k = \mathbf{I}\hat{\underline{z}}^E_{k-1} + \hat{\mathbf{B}}_k \hat{\underline{z}}^\Delta_k \ , \ \mathbf{C}^P_k = \frac{\mathbf{\Xi}_k}{1-\kappa} + \frac{\mathbf{\Gamma}_k}{\kappa} \ , \tag{14}$$

with $\mathbf{\Xi}_k = \mathbf{J}^E_k \mathbf{C}^E_{k-1} (\mathbf{J}^E_k)^T$, $\mathbf{\Gamma}_k = \hat{\mathbf{B}}_k \mathbf{C}^\Delta_k \hat{\mathbf{B}}^T_k$, for $0 < \kappa < 1$ (Schweppe, 1973). κ may be selected such that a measure of the "size" of Ω^P_k is minimized. An appropriate "size" measure is the volume of Ω^P_k, which is proportional to $\sqrt{\det(\mathbf{C}^P_k)}$. Minimizing the volume in three dimensions leads to the problem of determining the unique root of a fourth–order polynomial in $[0,1]$. The trace measure $\mathrm{tr}(\mathbf{C}^P_k)$, i.e., the sum of the main–diagonal elements of $\mathbf{C}^P_k$, is mathematically most convenient. It leads to the problem of determining the unique root of a second–order polynomial in $[0,1]$ irrespective of the problem dimensionality. Unfortunately, its meaning is questionable for the problem at hand, where x^P_k, y^P_k and ψ^P_k differ by some orders of magnitude. A more meaningful "size" measure leading to a minimization procedure of intermediate complexity is given by the trace measure of the projection of Ω^P_k onto the xy–plane multiplied by the square of half of the projection of Ω^P_k onto the ψ–axis. This is equivalent to $\mathrm{M}_{C^P_k C^P_k}$ with

$$\mathrm{M}_{AB} = \mathrm{tr}\left(\mathrm{proj}_{xy}(\mathbf{A})\right) \mathrm{proj}_{\psi}(\mathbf{B}) \ , \tag{15}$$

where $\mathrm{proj}_{SS}(\mathbf{C})$ is defined by eliminating those rows and columns from $\mathbf{C}$ that are not associated with the considered subspace SS. The minimizing κ is given by the unique root of

$$K_3\kappa^3 + K_2\kappa^2 + K_1\kappa + K_0 \tag{16}$$

in $[0,1]$ where

$$\begin{aligned} K_3 &= 2[\mathrm{M}_{\Xi_k\Xi_k} + \mathrm{M}_{\Gamma_k\Gamma_k} - \mathrm{M}_{\Xi_k\Gamma_k} - \mathrm{M}_{\Gamma_k\Xi_k}] \\ K_2 &= 3[\mathrm{M}_{\Xi_k\Gamma_k} + \mathrm{M}_{\Gamma_k\Xi_k} - 2\mathrm{M}_{\Gamma_k\Gamma_k}] \\ K_1 &= 6\mathrm{M}_{\Gamma_k\Gamma_k} - \mathrm{M}_{\Xi_k\Gamma_k} - \mathrm{M}_{\Gamma_k\Xi_k} \\ K_0 &= -2\mathrm{M}_{\Gamma_k\Gamma_k} \ . \end{aligned} \tag{17}$$

The proof is straightforward and consists of differentiating the "size" measure with respect to κ and setting the result to zero.

4.2. *Measurement*

The measurement equation for a single α_k at time k and an associated landmark at x^{LM}, y^{LM}

$$\sin(\alpha_k + \psi^M_k)\{x^{\mathrm{LM}} - x^M_k\} \\ = \cos(\alpha_k + \psi^M_k)\{y^{\mathrm{LM}} - y^M_k\} \tag{18}$$

is linearized around the predicted posture $\hat{\underline{z}}^P_k$, the measured angle $\hat{\alpha}_k$, and the nominal landmark position $\hat{x}^{\mathrm{LM}}$, $\hat{y}^{\mathrm{LM}}$. This yields $r_k = \underline{D}^T_k \underline{z}^M_k + e_k$ with

$$
\begin{aligned}
r_k &= c_k^1 \hat{x}^{LM} - c_k^2 \hat{y}^{LM} - c_k^3 \hat{\psi}_k^P \\
\underline{D}_k &= (c_k^1, -c_k^2, -c_k^3)^T \\
e_k &= (-c_k^1, c_k^2)(\Delta x^{LM}, \Delta y^{LM})^T - c_k^3 \Delta\alpha \ .
\end{aligned} \tag{19}
$$

The constants are defined as $c_k^1 = \sin(\hat{\alpha} + \hat{\psi}_k^P)$, $c_k^2 = \cos(\hat{\alpha} + \hat{\psi}_k^P)$, and $c_k^3 = c_k^2\{\hat{x}^{LM} - \hat{x}_k^P\} + c_k^1\{\hat{y}^{LM} - \hat{y}_k^P\}$. e_k can thus be bounded, i.e., $|e_k| < e_k^{max}$ with

$$
e_k^{max} = \sqrt{\begin{pmatrix} -c_k^1 \\ c_k^2 \end{pmatrix}^T \mathbf{C}^{LM} \begin{pmatrix} -c_k^1 \\ c_k^2 \end{pmatrix}} + |c_k^3|\delta_\alpha \tag{20}
$$

Two equivalent representations of the measurement set will be given in the following. The first consists of two boundary planes given in normalized Hesse form as

$$
\underline{N}_k^T \underline{z}_k^M + t_k^1 = 0, \ \underline{N}_k^T \underline{z}_k^M + t_k^2 = 0 \tag{21}
$$

with

$$
\underline{N}_k = -\frac{\underline{D}_k}{\|\underline{D}_k\|}, \ t_k^1 = \frac{r + e_{max}}{\|\underline{D}_k\|}, \ t_k^2 = \frac{r - e_{max}}{\|\underline{D}_k\|} \tag{22}
$$

The second representation is

$$
\Omega_k^M = \{\underline{z}_k^M : |\underline{A}_k^T \underline{z}_k^M - b_k| \leq 1\} \ . \tag{23}
$$

They may be converted into each other via $\underline{A}_k = 2\underline{N}_k/(t_k^2 - t_k^1)$, $b_k = -(t_k^2 + t_k^1)/(t_k^2 - t_k^1)$.

4.3. *Robust Combination of Information*

Conceptionally, fusion just consists of calculating the intersection of the sets Ω_k^P, Ω_k^M. Ω_k^P is the ellipsoidal set of predicted postures, Ω_k^M is the measurement strip. The intersection of the two sets Ω_k^P, Ω_k^M is not in general again an ellipsoid. To arrive at a recursive scheme, an ellipsoid circumscribing the intersection is required. A bounding ellipsoid is given by (Sabater and Thomas, 1991)

$$
\begin{aligned}
\Omega_k^E &= \{\underline{z}_k^E : (\underline{z}_k^E - \hat{\underline{z}}_k^E)\,(\mathbf{C}_k^E)^{-1}\,(\underline{z}_k^E - \hat{\underline{z}}_k^E)^T\} \\
\mathbf{C}_k^E &= K_k \mathbf{C}_k^0 \\
\mathbf{C}_k^0 &= \mathbf{C}_k^P - \lambda \frac{\mathbf{C}_k^P \underline{A}_k \underline{A}_k^T \mathbf{C}_k^P}{1 + \lambda G_k} \\
\hat{\underline{z}}_k^E &= \hat{\underline{z}}_k^P + \lambda \mathbf{C}_k^0 \underline{A}_k \epsilon_k \\
\epsilon_k &= b_k - \underline{A}_k^T \hat{\underline{z}}_k^P \\
G_k &= \underline{A}_k^T \mathbf{C}_k^P \underline{A}_k \\
K_k &= 1 + \lambda - \lambda\epsilon_k^2/(1 + \lambda G_k)
\end{aligned} \tag{24}
$$

for all $\lambda \geq 0$. This set has the interesting property that it both contains the intersection of the measurement and the prediction set and is itself contained in their union, i.e.,

$$
(\Omega_k^M \cap \Omega_k^P) \subset \Omega_k^E \subset (\Omega_k^M \cup \Omega_k^P) \ . \tag{25}
$$

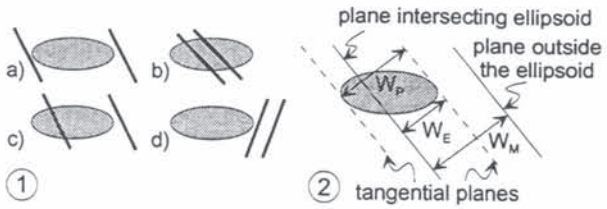

Fig. 1. 1: Configurations for strip and ellipsoid (2D). 2: Definitions for assessing consistency.

The non–linear fusion comprises 4 cases:

- **No uncertainty reduction:** The actual measurement is of no help in reducing the uncertainty, Fig 1.1 a).
- **Consistency:** Both planes defining the measurement set intersect the ellipsoidal prediction set, Fig. 1.1 b).
- **Partial consistency:** Only one plane intersects the prediction set, Fig. 1.1 c).
- **Inconsistency:** Prediction set Ω_k^P and measurement set Ω_k^M do not share a common point, Fig. 1.1 d).

For the case of (partial) consistency of ellipsoid and strip, the *volume* of the bounding ellipsoid in (24) may be minimized by selecting the weight λ as the most positive root of the quadratic equation given by (Sabater and Thomas, 1991)

$$
\begin{aligned}
&(N-1)G_k^2\lambda^2 + (2N - 1 + \epsilon_k^2 - G_k)G_k\lambda \\
&+N(1-\epsilon_k^2) - G_k = 0 \ ,
\end{aligned} \tag{26}
$$

where N is the dimension, here $N = 3$. This result is now generalized to obtain an EBS with a *minimum volume projection* onto an arbitrary subspace. λ_{OPT} is the positive real root of

$$
\begin{aligned}
&\lambda^3(G_k - H_k)G_k^2 L + \lambda^2\{L(3G_k - 2H_k) - H_k\}G_k \\
&+ \lambda\{[3G_k - H_k + \epsilon_k^2(H_k - G_k)]L \\
&- G_k H_k - H_k + \epsilon_k^2 H_k\} + L(1 - \epsilon_k^2) - H_k \ ,
\end{aligned} \tag{27}
$$

with L the subspace dimension and

$$
H_k = \underline{A}_k^T (\bar{\mathbf{C}}_k^P)^T [\mathrm{proj}(\mathbf{C}_k^P)]^{-1} \bar{\mathbf{C}}_k^P \underline{A}_k^T \ . \tag{28}
$$

$\bar{\mathbf{C}}_k^P$ is obtained from $\mathbf{C}_k^P$ by eliminating the rows not associated with the considered subspace. The proof is patterned after the one in (Deller Jr and Luk, 1989) and is sketched in the appendix. Application of this concept to the localization problem leads to a tailor–made bounding operation. The inherently high precision of the orientation estimate ψ^E compared to the position estimate x^E, y^E is considered by minimizing the projection of the EBS onto the x, y subspace. The resulting EBS is more conservative in ψ^E, but tight for the more critical position estimate x^E, y^E.

Using the optimal EBS is successful as long as the model is exact. However, modeling errors may

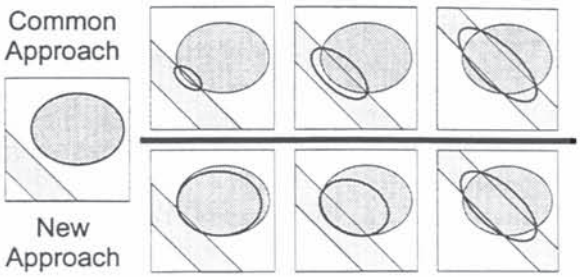

Fig. 2. EBSs for the intersection of ellipsoid and strip. Top: Common scheme. Bottom: Extension employing consistency measures.

lead to an unreasonably small estimation set Ω_k^E. Enhanced robustness is achieved by imposing a higher priority on the set of predicted states Ω_k^P since it contains the information obtained from all the past measurements. This priority should depend on the degree of consistency of the two sets Ω_k^P and Ω_k^M. Roughly speaking, the idea is to select the set Ω_k^E such that it exhibits a growing tendency towards the prediction set Ω_k^P with falling degree of consistency of the sets Ω_k^P and Ω_k^M. Referring to Fig. 1.2, a reasonable consistency measure is given by the intersection width W_E divided by the geometric mean of the strip width W_M and the ellipsoid width W_P

$$\mathrm{CM}(\Omega_k^P, \Omega_k^M) = \frac{W_E}{\sqrt{W_P W_M}}, \; 0 \leq \mathrm{CM} \leq 1 \,. \quad (29)$$

λ in (24) is selected from $[0, \lambda_{\mathrm{OPT}}]$ as an appropriate function of the consistency measure. A shifted logistic function

$$\lambda = \lambda_{\mathrm{OPT}} / [1 + \exp(-S(\mathrm{CM} - M))] \,, \quad (30)$$

is used with S, M chosen as $S = 10$, $M = 0.5$. The influence of this extension on the fusion result is demonstrated in Fig. 2 by comparing it with the common approach for four cases. For the common approach, the volume of the resulting EBS Ω_k^E experiences large changes when the measurement set just changes slightly. Single (unmodeled) measurement outliers lead to an extremely small EBS. On the other hand, the new approach calculates Ω_k^E by modifying Ω_k^P depending on its consistency with Ω_k^M. Thus, single erroneous measurements have a reduced impact on the fusion result.

A schematic overview of the proposed scheme for localization during fast motion based on angle measurements is depicted in Fig. 3. The feedback of $\hat{\underline{z}}_k^E$ to the process for determination of Ω_k^M deserves some attention. It may replace $\hat{\underline{z}}_k^P$ to iteratively refine the linearization of (18). The scheme may easily be parallelized into three tasks: The fusion loop, the determination of landmarks not occluded by partitioning walls, and dead–reckoning.

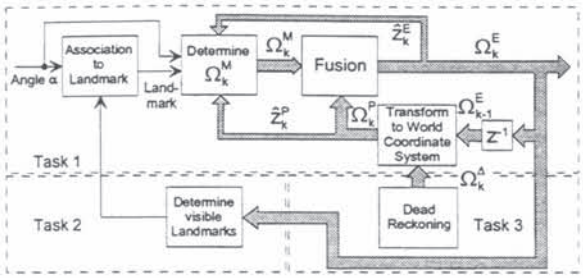

Fig. 3. Scheme of set theoretic recursive estimator.

5. EXPERIMENTAL VALIDATION

The effectiveness of the new approach is demonstrated by navigating a fast (2 m/sec) omnidirectional service robot (Hanebeck and Schmidt, 1994) through an office environment. An onboard laser–based goniometer takes angular measurements on retro–reflecting tape strips attached to the walls as artificial landmarks. 20 horizontal 360^o–scans per second are performed; absolute accuracy is about 0.02^o. Thus, the predominant uncertainties result from inaccurate knowledge about the positions of the fixed landmarks. A map contains nominal positions of 22 identical landmarks and partitioning walls, Fig. 4. The full scale robot is equipped with three independently steerable drive wheels. Dead–reckoning based on these wheels suffers from error sources like imperfect wheel coordination and uncertain wheel/floor contact points. The usual white Gaussian noise model is not appropriate here. The amplitude–bounded nature of the correlated error sources suggests the proposed set theoretic treatment. Once initialized with the algorithm introduced in Sec. 3, the robot performs 10 cycles of a predefined course, Fig. 4. The localization estimate based on the fusion of goniometer data and dead–reckoning is compared with data from dead–reckoning only. The highly correlated nature of the accumulating dead–reckoning errors is obvious. On the other hand, the vehicle is kept very accurately on track with the localization estimate. Absolute accuracy has found to be about ± 2 cm and $\pm 0.5^o$.

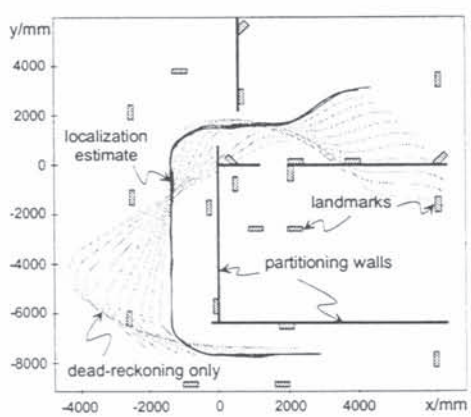

Fig. 4. Experimental in–motion localization.

6. CONCLUSION

Set theoretic concepts have been applied to posture estimation of fast–moving mobile robots which perform angular measurements on the location of known but undistinguishable landmarks. In this context, four main results are presented:
1) A simple *closed–form* solution for the robot position given angular locations of N known landmarks is derived, which consists of $N-1$ equations *linear* in the position.
2) Consistency measures for assessing the consistency of candidate posture sets are introduced to design set theoretic estimators which are robust to modeling errors.
3) The common minimum volume EBS algorithms for the intersection of an ellipsoid and a strip are extended to obtain the EBS with *minimum volume projection* onto an arbitrary subspace. Application to the localization problem allows consideration of the inherently higher precision in orientation ψ by selecting the EBS with *minimum volume projection* onto the xy–plane. This EBS bounds the exact estimation set more tightly in x, y and is more conservative in ψ.
4) A scheme for approximate propagation of an ellipsoidal posture set with set valued data from an uncertain dead–reckoning system is given, which just involves finding the roots of a third–order polynomial.
The effectiveness of the proposed set theoretic estimator has been demonstrated by experiments with a fast omnidirectional service robot. The full scale robot is equipped with a laser–based goniometer which makes angular measurements on the location of tape strips attached to the wall as artificial landmarks. Navigation in an office environment revealed a high absolute accuracy of about ± 2 cm and $\pm 0.5^0$.

7. REFERENCES

Betke, M. and L. Gurvits (1994). Mobile Robot Localization Using Landmarks. In: *Proc. of the 1994 IEEE/RSJ/GI Int. Conf. on Intelligent Robots and Systems, Munich, Germany.* pp. 135–142.

Deller Jr, J. R. and T. C. Luk (1989). Linear Prediction Analysis of Speech Based on Set–Membership Theory. *Computer Speech and Language* **3**, 301–327.

Drumheller, M. (1987). Mobile Robot Localization Using Sonar. *IEEE Trans. on PAMI* **9**(2), 325–332.

Grimson, W. E. L. and T. Lozano-Pérez (1985). Recognition and Localization of Overlapping Parts From Sparse Data in Two and Three Dimensions. In: *Proc. of the 1985 IEEE Int. Conf. on Robotics and Automation, St. Louis, MO.* pp. 61–66.

Hanebeck, U. D. and G. Schmidt (1994). A New High Performance Multisonar System for Fast Mobile Robots. In: *Proc. of the 1994 IEEE/RSJ/GI Int. Conf. on Intelligent Robots and Systems, Munich, Germany.* pp. 1853–1860.

Nishizawa, T., A. Ohya and S. Yuta (1995). An Implementation of On–board Position Estimation for a Mobile Robot. In: *Proc. of the 1995 IEEE Int. Conf. on Robotics and Automation, Nagoya, Japan.* pp. 395–400.

Sabater, A. and F. Thomas (1991). Set Membership Approach to the Propagation of Uncertain Geometric Information. In: *Proc. of the 1991 IEEE Int. Conf. on Robotics and Automation, Sacramento, CA.* pp. 2718–2723.

Schweppe, F. C. (1973). *Uncertain Dynamic Systems.* Prentice–Hall.

Sutherland, K. T. and W. B. Thompson (1994). Localizing in Unstructured Environments: Dealing with the Errors. *IEEE Trans. on Robotics and Automation* **10**(6), 740–754.

Tsumura, T., H. Okubo and N. Komatsu (1993). A 3-D Position and Attitude Measurement System Using Laser Scanners and Corner Cubes. In: *Proc. of the 1993 IEEE/RSJ Int. Conf. on Intelligent Robots and Systems, Yokohama, Japan.* pp. 604–611.

Wiklund, U., U. Andersson and K. Hyyppä (1988). AGV Navigation by Angle Measurements. In: *Proc. of the 6th Int. Conf. on Automated Guided Vehicle Systems, Brussels, Belgium.* pp. 199–212.

8. APPENDIX

Proof of (27): The projection of $\mathbf{C}_k^E$ onto a certain subspace is denoted as $\text{proj}(\mathbf{C}_k^E)$ and may be written as

$$K_k \,\text{proj}(\mathbf{C}_k^P) - \lambda K_k \frac{\text{proj}(\mathbf{C}_k^P \underline{A}_k \underline{A}_k^T \mathbf{C}_k^P)}{1+\lambda G_k} \quad . \tag{31}$$

The volume of $\text{proj}(\mathbf{C}_k^E)$ is proportional to

$$\det\left(K_k \mathbf{I} - \lambda K_k \frac{[\text{proj}(\mathbf{C}_k^P)]^{-1} \bar{\mathbf{C}}_k^P \underline{A}_k \underline{A}_k^T \bar{\mathbf{C}}_k^P}{1+\lambda G_k}\right) \tag{32}$$

where $\bar{\mathbf{C}}_k^P$ is defined as $\mathbf{C}_k^P$ with the rows not associated with the subspace eliminated. Applying the matrix identity (Deller Jr and Luk, 1989)

$$\det(c\mathbf{I} + \underline{y}\underline{z}^T) = c^{L-1}(c + \underline{y}^T \underline{z}) \quad , \tag{33}$$

where L is the subspace dimension, (32) becomes

$$K_k^L \frac{1+\lambda(G_k - H_k)}{1+\lambda G_k} \quad , \tag{34}$$

with H_k from (28). Differentiating with respect to λ and setting the result to zero yields (27).